International Journal of Impact Engineering 36 (2009) 940–947

Contents lists available at ScienceDirect

International Journal of Impact Engineering

journal homepage: www.elsevier.com/locate/ijimpeng

Laboratory-scale techniques for the measurement of a material response to an explosive blast

M.J. Hargather*, G.S. Settles

Mechanical and Nuclear Engineering, The Pennsylvania State University, 301D Reber Building, University Park, PA 16802, USA

ARTICLE INFO

Article history:
Received 9 June 2008
Received in revised form
10 December 2008
Accepted 14 December 2008
Available online 25 December 2008

PACS:
81.70.Bt

Keywords:
Explosive
Blast testing
Laboratory-scale
Plate deformation

ABSTRACT

Laboratory-scale experiments were performed to measure the deformation of thin plates in response to varying explosive impulse. Experiments were conducted with a known explosive mass suspended in air at a known distance from an aluminum witness plate clamped in a "shock-hole" fixture. Through the use of well-characterized PETN and TATP explosive charges, the explosive impulse applied to each witness plate was determined a priori. The witness-plate response was measured using high-speed digital cameras to determine time-resolved, three-dimensional surface motion and maximum plate deformation. The results show that the maximum dynamic plate deformation is a straightforward function of applied explosive impulse, as determined from the explosive characterization. The experimental trend is the same despite the two different explosives used, highlighting that explosive impulse, determined through a blast characterization, is the controlling parameter in material blast response. A new experimental technique is used here to measure the dynamic blast response and the experimental errors are documented. Ultimately, applications of laboratory-scale explosive testing to computational code validation, material response scaling, and high-speed material property definition are discussed.

1. Introduction

Explosive blast research is important in understanding the damage caused by an explosion and also for the development of blast-resistant materials. Typically, explosive blast tests are conducted on full-scale models or structures to determine the actual material response [1]. Even the smallest of these full-scale tests can require 10–100 kg explosive charges at distances of up to 100 m from the test article, which forces these tests outdoors into relatively uncontrolled settings [2]. At this scale, instrumentation becomes difficult and expensive, often yielding only point-wise piezoelectric pressure profiles at limited locations and a qualitative rather than quantitative evaluation of material deformation. Optical methods to reveal shock waves in such field testing, such as background distortion and sunlight shadowgraphy, are often crude and weather-dependent [3]. Overall, the instrumentation difficulties and prohibitive cost of large-scale blast testing often result in limited experiments and even-more-limited data. Although not able to completely eliminate full-scale testing, laboratory-scale experiments nonetheless provide unique data collection opportunities and new insights into the physical phenomena.

The majority of the published laboratory-scale research focuses on how a "witness plate" is deformed due to an explosive blast. These tests typically result in post-test measurements of maximum plate deflection and qualitative plate shape [4]. Nurick et al. performed the majority of the initial work and established standard terms for the qualitative categorization of witness-plate failures into one of three modes [5]. Dynamic deformation measurements were also performed, with the simplest methods producing point measurements of witness-plate deflection as a function of time [6,7]. Other methods use strain gages to measure strain rates at specified locations on the surface of the material [8]. Optical methods, however, provide the unique ability to measure deformation without contacting the plate surface. A method developed by Nurick and Martin [9], determined plate deformation by measuring when the plate surface disrupted a laser beam parallel to the initial plate surface, but was limited to determining maximum deflection and not surface shape. More recent methods, including those used by Espinosa et al. [10,11], use laser interference and Moire patterns to determine time-resolved, three-dimensional material deformations and shapes. The optical technique evaluated by Siebert et al. [12] and used by Fourney et al. [13,14] and Tiwari et al. [15] is capable of measuring time-resolved, three-dimensional

* Corresponding author.
E-mail addresses: mjh340@psu.edu (M.J. Hargather), gss2@psu.edu (G.S. Settles).

0734-743X/$ – see front matter © 2008 Elsevier Ltd. All rights reserved.
doi:10.1016/j.ijimpeng.2008.12.008

surface shapes by using two high-speed digital cameras in stereo and digital image correlation software. This non-contact optical method is simple to implement and requires only optical access to the deforming surface, and thus is used in the present research.

Although previous experimental investigations have developed complex methods for measuring plate deformation, they suffer a lack of full knowledge of the explosive energy input and explosive impulse. Explosive impulse is defined as the integral of shock wave overpressure with respect to time, and represents momentum associated with the shock wave propagation. When a shock wave impinges upon a witness plate, a portion of this momentum is transfered to the plate, resulting in plate motion and deformation. Determining the exact momentum imparted to the plate, however, is difficult and depends upon plate physical properties and deformation response.

Bodner and Symonds [16] developed a ballistic pendulum method to estimate the explosive impulse applied to plates in laboratory blast experiments. Through an energy balance, the ballistic pendulum method estimates the explosive impulse from the change in height of a free-swinging mass [17]. It does not, however, directly measure the primary shock wave energy applied to a witness plate, but rather a total energy impulse delivered to the ballistic pendulum fixture over the entire event. This measurement neither directly accounts for variations in shock strength and overpressure duration, nor does it discriminate between positive and negative blast impulses.

The accurate measurement of the explosive impulse applied to a witness plate is further complicated, in the previous research, by the frequent use of a foam insert between the explosive and plate [16,18]. Foam inserts were used to modify the blast parameters to prevent the plates from failing in shear [16]. This modification of the blast parameters, however, changes the impulse shape and ultimately the resulting plate deformation in ways that are not simple to understand. The actual plate loading conditions cannot be measured in these laboratory-scale experiments, and therefore cannot be directly extrapolated to actual full-scale air-blast experiments.

The present research presents a new method for conducting witness-plate blast deformation experiments in the laboratory. The present method uses explosives that have been characterized using the high-speed optical method of Hargather and Settles [19] and Kleine et al. [20]. By way of this characterization procedure, the shock wave explosive impulse is known as a function of radius from the charge. A charge of known mass is then exploded at a known stand-off distance from the witness plate and the dynamic, time-resolved, three-dimensional material deformation is measured using twin high-speed cameras. The explosive energy from the charge is thus coupled to the witness plate through the air. In this manner, the explosive impulse delivered to the plate via the shock wave is well known and representative of typical blast-loading scenarios.

2. Experimental methods

The primary objective of the present research is to develop the techniques required for measuring material responses to explosive impulses. This research is dependent on accurate characterization of the explosives used and on precise measurement of material deformation. A characterized explosive is exploded at a known distance from a thin aluminum plate, deforming the plate due to explosive impulse. Optical image correlation is used to measure the time-resolved, three-dimensional surface shape of the deforming plate throughout the explosive event. Aluminum alloy 3003, 0.406 mm thickness, was used here as the witness-plate material. The aluminum was purchased from McMaster-Carr, Inc., and had quoted yield strength of 144.8 MPa and a Brinell hardness of 40, meeting manufacturing standard ASTM B209.

2.1. Shock-hole fixture

A single witness plate of aluminum is bolted into a "shock-hole"[1] fixture, as shown in Fig. 1. The exposed portion of the aluminum plate is a 0.25 m diameter circle which is centered on the plate. The rest of the plate remains firmly clamped within the shock-hole fixture by the 12 symmetrically-arranged bolts, which are hand-tightened with a wrench. This fixture eliminates all visible plate wrinkling at the clamped boundary and prevents slippage from the clamped region into the exposed, circular measurement area. The effect of the clamp depth on the applied impulse was not considered here, since recent work by Bonorchis and Nurick showed that clamp depth did not influence the maximum plate deformation [21]. The entire shock-hole fixture is mounted vertically, 1.2 m above the floor on the edge of a rigid platform, in the center of a 12.2×13.7 m room where shock reflections can be ignored.

The witness-plate fixture was also designed to provide the optical access required to make deformation measurements, as described in Section 2.2. The complete setup for the present material deformation research is shown in Fig. 2. The plate fixture location relative to the cameras is fixed and the "stand-off distance" from the plate surface to the center of the explosive charge is a primary variable. As the stand-off distance is changed, the explosive impulse applied to the plate is varied, as discussed in Section 2.3. The face of the plate nearest the explosive will be referred to as the "front" of the plate and the "back" will indicate the face being imaged by the cameras.

2.2. Optical deformation measurement

Vic-3D software by Correlated Solutions Inc. is used in the present research to measure witness-plate deformation [22]. This software uses simultaneous images from two cameras in parallax to mathematically define a surface of arbitrary shape, here the backside of the witness plate. With the use of two high-speed Photron APX-RS digital video cameras, a time-resolved record of plate shape history can be created and deformation data thus extracted. For the current research, deformation refers to the change in the measured out-of-plane plate position relative to a reference position defined before any explosive loading occurs.

The first step in using this software is to perform a calibration for the orientation of the two cameras relative to each other and to the field-of-view. The cameras must be positioned so that they both image the desired field-of-view, in this case the backside of the witness plate. The cameras are placed at an angle, β, relative to one another as shown in Fig. 2. The stereo calibration accounts for this primary stereoscopic angle and also the corresponding angles in the two other orthogonal planes, all of which are approximately zero in the present research. The angle β between the cameras is in the range of 20–40°, which maximizes the measurement sensitivity for the software used here.

Once calibrated, the software is able to interpret where in space an object is located, based on its appearance from the two camera perspectives. In order to make measurements on a witness-plate surface, the surface is painted with a high-contrast random dot pattern. The random dot pattern provides unique details across the

[1] The term "shock-hole" originates from the US Army Aberdeen Test Center, where such a fixture is used to test explosive perforation or "holing" of witness plates. In the present research, however, such material failure does not occur.

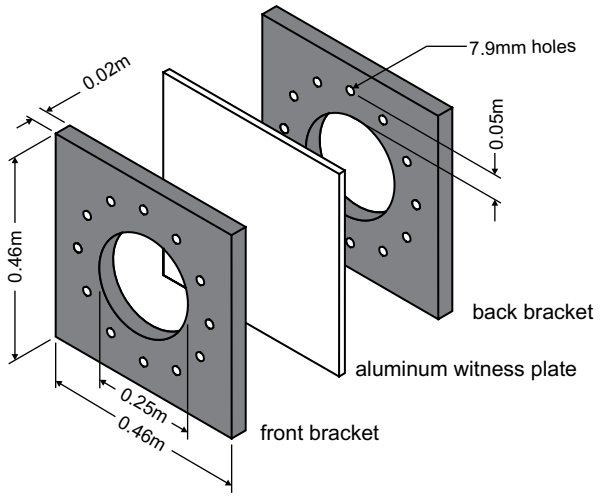

Fig. 1. Schematic of the "shock-hole" fixture used to support aluminum witness plates for each experiment.

surface that can be identified and analyzed by the software. The random dot pattern is spray-painted onto the backside of each aluminum witness plate before it is placed into the test fixture. The dot pattern should have many dots, each occupying an area of approximately 5 camera pixels, across the field to be analyzed.

Fig. 3 shows a typical dot pattern on a witness-plate surface as seen from the two cameras. The field-of-view shown is typical of all present experiments, and focuses on the centerline of the plate as discussed in Section 3.1. The circular shock-hole plate fixture edge can be seen in the images, with horizontal fiducial marks on the fixture to indicate the horizontal diameter of the opening. By imaging this field-of-view, each experiment thus produces temporally-resolved witness-plate deformation data for the central plate diameter, which are analyzed to determine maximum deformation.

The plate fixture is illuminated with three 600 W continuous Calumet flood lights. The lights are positioned at oblique angles to the plate surface to decrease glare reflection from the plate into the camera lenses. The illumination was experimentally chosen to fully and evenly illuminate the plate surface and allow camera shutter speeds as short as 4 μs, thus minimizing image blur during the explosive event. Greater illumination, if available, would allow a decrease in lens aperture and possibly a further increase in shutter speed. Trial-and-error methods with the dot pattern show that black dots on a white field require less illumination than the opposite, and are therefore used throughout the present work. Illumination requirements change with field-of-view, choice of lens, and *f*-stop setting.

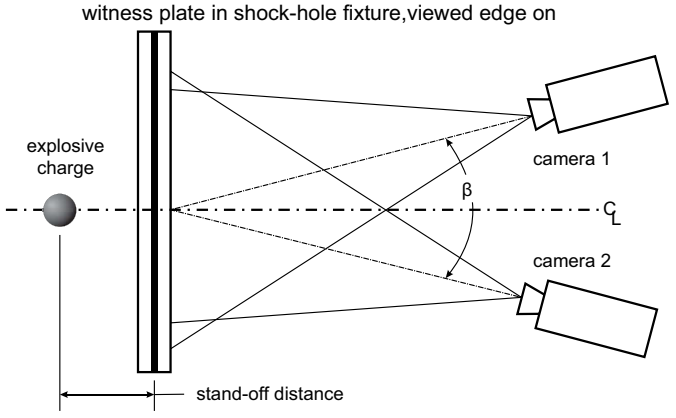

Fig. 2. Experimental setup for material deformation experiments, top view.

2.3. Explosive charges

Well-characterized explosive charges are used, so that the explosive loading of each witness plate is accurately known. Two different explosives, pentaerythritol tetranitrate (PETN) and triacetone triperoxide (TATP), are used here because of their previous characterizations [19,23]. In the previous work we documented the shock propagation Mach number versus radius from the charge center, thus the maximum overpressure versus radius, for both PETN and TATP. The characterization also yielded the overpressure duration versus radius for each explosive. Thus explosive impulse is approximately known as a function of radial distance from a charge. Further information on charge initiation, repeatability, and the entire characterization procedure can be found in the previous work of Hargather and Settles [19].

Explosive impulse, defined as the integral of pressure with respect to time, has been shown to be an important parameter for blast research [24]. A schematic of the pressure-time history of an explosively-driven shock wave is shown in Fig. 4. The area labeled as the "actual impulse" is the area under the true pressure profile. For the present research, a triangular impulse approximation is used [25]. This approximation is used for simplicity because the exact pressure decay profile is not known, but the maximum pressure, P_0, and the overpressure duration, t_d, are known from the explosive characterization [19]. This approximation somewhat over-estimates the impulse, but does not change the fundamental relationships reported here; using the exact impulse, if known, would only change slightly the slope of the impulse-deformation curves presented below. The negative impulse, at $t \geq t_d$, is ignored in the present research [25].

Experiments performed here couple the energy from the exploding charge to the witness plate via the air. The explosively-driven shock propagates through the air and applies an explosive impulse to the plate surface. The explosive impulse applied to the witness plate is varied by changing the explosive material, its mass, or its stand-off distance. Explosive impulse variation as a function of radius has been previously determined in our work for PETN and TATP [19,23], and is shown here in Fig. 5. Charge masses ranged from 0.5 to 1.1 g, with stand-off distances from 0.03 to 0.15 m, as given in Tables 1 and 2. The range of charge masses and stand-off distances was within the limits of blast scalability and repeatability as previously demonstrated [19].

Using the Sachs scaling law [26], each actual charge mass and atmospheric test conditions are scaled to a 1 g, normal temperature and pressure reference value so that the impulses can be determined. The radius required for the desired impulse is then determined from Fig. 5. This radius is then re-scaled, according to Sachs scaling, to determine the charge stand-off distance for the current experiment. In this manner, the maximum explosive impulse applied to the plate center is known for an explosive charge of any mass at a given stand-off distance. The average impulse applied to the plate can also be determined through a similar integration procedure, wherein the distance from the charge center to a given location on the plate is used as the radius in Fig. 5.

3. Experimental results

3.1. Deformation symmetry

At high frame rates, the Photron APX-RS digital camera pixel resolution is insufficient to measure the entire witness-plate surface motion at once. Thus, only a central strip of the plate surface

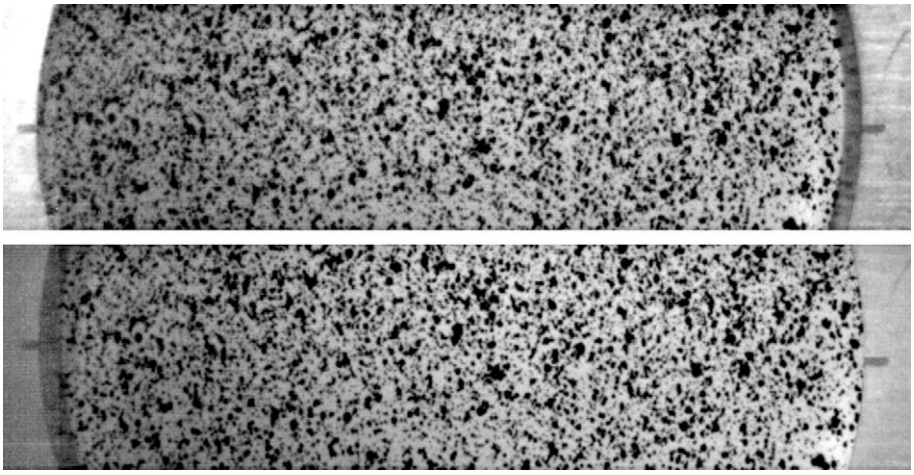

Fig. 3. Typical image pair showing the random dot pattern and field-of-view for a standard experiment, the distance between the horizontal marks on the shock-hole fixture is approximately 0.25 m.

is actually measured in order to allow the required frame rate and spatial resolution to properly capture the plate motion. For the present research, the horizontal diameter of the exposed plate surface is centered within the field-of-view and approximately 0.03 m of the plate surface above and below this diameter is imaged, as shown in Fig. 3. This strip-wise view conforms to the Photron APX-RS camera's rectangular field-of-view capability at high frame rates.

Before limiting the field-of-view to this region, however, experiments were performed to measure the degree of symmetry of the witness-plate deformation. In these experiments the cameras imaged the entire exposed plate surface and recorded its motion at 10,000 frames per second (fps). At this frame rate the pixel resolution is 512×512, providing the same horizontal resolution as the higher frame rate used for the primary measurements. At 36,000 fps, the primary measurement frame rate, the frame resolution is 512×128, providing an optimum spatial and temporal resolution balance in order to image a central strip of the witness plate in the test fixture with the present cameras.

Fig. 6 shows out-of-plane deformation contours at the time of maximum deformation from one of the full-field experiments. Also shown in Fig. 6 are four diameters, numbered 1–4 which are used to measure the deformation symmetry. Fig. 7 shows the deformation recorded along each of the 4 diameters. As shown in Figs. 6 and 7, the plate deformation during an experiment is highly radially-symmetric; all 4 diameters show almost the same shape and maximum deformation. Thus, only a central strip of the exposed witness-plate area is imaged in all subsequent experiments, and symmetry is assumed.

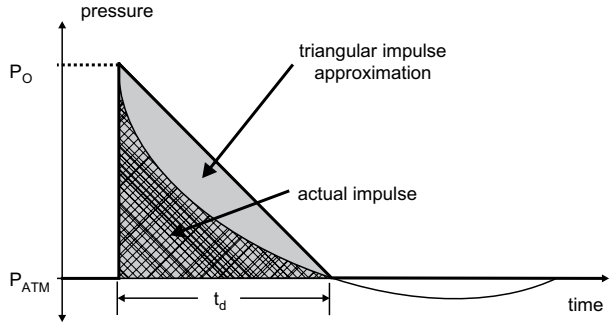

Fig. 4. Pressure-time history of an ideal, explosively-driven shock wave showing actual and triangular approximation of explosive impulse.

Even though radial symmetry is assumed, it was found that the point of maximum deformation does not always occur perfectly centered on the plate, as seen in Fig. 7. These small variations occur if the explosive charge is not perfectly pre-positioned. If only a single radius of the plate deformation is measured, this small variability can cause data reduction to become problematic, and can potentially lose information about the deformation process. However, by recording a central strip, the center of the witness plate can easily be located using fiducial marks on the plate fixture. Subsequent experiments determined that small variations in maximum deformation location did not affect the magnitude of the deflection data; in the data presented, the maximum deformation point occurred at an average distance of 8.7 mm from the plate center. This variability is approximately 3.5% of the plate diameter, thus is accepted to be within the estimated experimental error.

Fig. 6 also shows minor regions where the Correlated Solutions software was unable to perform a correlation, such as at the lower left extremity of the exposed region. During an experiment, such errors can occur when the plate surface loses paint locally or becomes over- or under-exposed. Local paint loss can result from fragment impact or from large local deformations. If the area of interest is thus adversely affected and no correlation is possible, then the data set must be rejected (though this is rare). Uniform

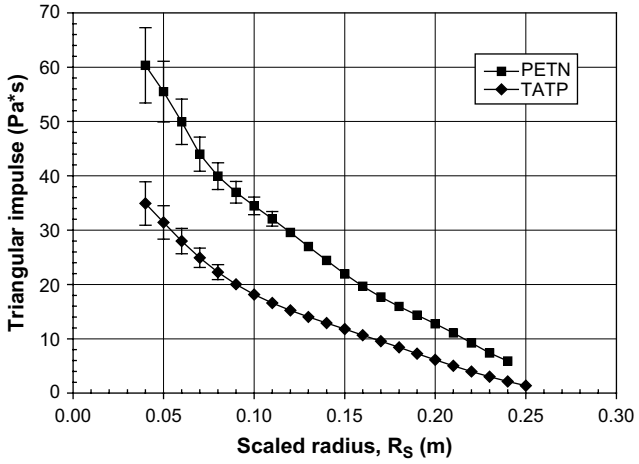

Fig. 5. Experimentally-determined triangular explosive impulse versus radius for 1 g PETN and TATP charges [19,23].

Table 1
Summary of material deformation experiments using PETN.

Test	Charge mass (g)	Stand-off distance (m)	Incident impulse		Maximum dynamic plate deformation (mm)
			Maximum (Pa s)	Average (Pa s)	
1	0.90	0.115	28.8	21.4	7.55
2	0.64	0.080	31.2	21.7	7.80
3	0.74	0.090	31.3	22.5	8.49
4	0.75	0.075	35.5	25.3	10.51
5	1.02	0.091	37.1	28.3	11.51
6	0.89	0.080	37.4	27.6	11.10
7	1.00	0.085	38.4	29.0	10.94
8	0.65	0.060	38.4	25.2	10.20
9	0.70	0.060	40.1	26.5	10.54
10	0.59	0.050	42.1	25.2	9.98
11	0.98	0.070	43.5	31.2	12.49
12	0.85	0.055	48.7	31.1	11.77
13	0.90	0.050	55.1	33.2	14.09
14	0.82	0.035	57.0	34.3	15.41
15	0.88	0.035	58.6	35.9	16.57
16	0.90	0.035	59.1	36.4	16.20

illumination and careful paint application along with fragment-free explosive charges are important to maximize useful data collection. To improve paint adhesion to the aluminum plate, the surface is lightly roughened with 100-grit sandpaper prior to paint application.

3.2. Experimental error estimation

The experimental error of the plate deformation measurements is composed of the error in the measured plate deformation profile and the error due to shock-hole fixture motion during an experiment. The error associated with computing the plate surface shape from image data is primarily a function of the physical area imaged and the camera pixel resolution used. To estimate this error, sequential image pairs of the flat plate surface prior to explosive loading were examined. It was found that the calculated "deformation" between these image pairs amounted to approximately-random "noise" across the witness-plate surface. With the fixed camera resolution and camera-to-plate distance used here, it was determined that this experimental correlation error is approximately uniform and equal to ± 0.05 mm.

Shock-hole fixture motion was measured throughout the explosive event and after the event to evaluate vibrational and translational errors. It was determined that the fixture oscillation during the first 1 ms of deformation, during which the maximum plate deformation occurs here, was approximately ± 0.05 mm. The final fixture position was also determined to be within ± 0.05 mm of the original fixture position, indicating that the fixture does not have any significant translational motion during the event.

Through superposition, the total experimental error in all plate surface measurements was determined to be ± 0.10 mm. This error is applied to all dynamic deformation measurements, for all impulse conditions and for the camera position and resolution that remained fixed during the present experiments.

Table 2
Summary of material deformation experiments using TATP.

Test	Charge mass (g)	Stand-off distance (m)	Incident impulse		Maximum dynamic plate deformation (mm)
			Maximum (Pa s)	Average (Pa s)	
1	0.60	0.150	5.5	2.8	1.94
2	0.60	0.110	9.5	6.4	2.66
3	0.61	0.080	12.9	8.7	3.48
4	0.55	0.070	13.2	8.7	3.21
5	0.67	0.070	14.6	10.1	4.04
6	0.62	0.060	15.2	10.2	4.01
7	0.53	0.050	15.3	9.7	3.79
8	0.63	0.060	15.3	10.3	4.03
9	0.67	0.060	15.8	10.8	4.27
10	0.62	0.050	16.5	10.8	4.61
11	0.59	0.040	17.5	11.0	4.83
12	0.55	0.030	18.5	11.0	5.42
13	0.69	0.040	18.8	12.2	5.14
14	0.65	0.030	19.9	12.2	5.16
15	0.72	0.030	20.7	13.0	6.65

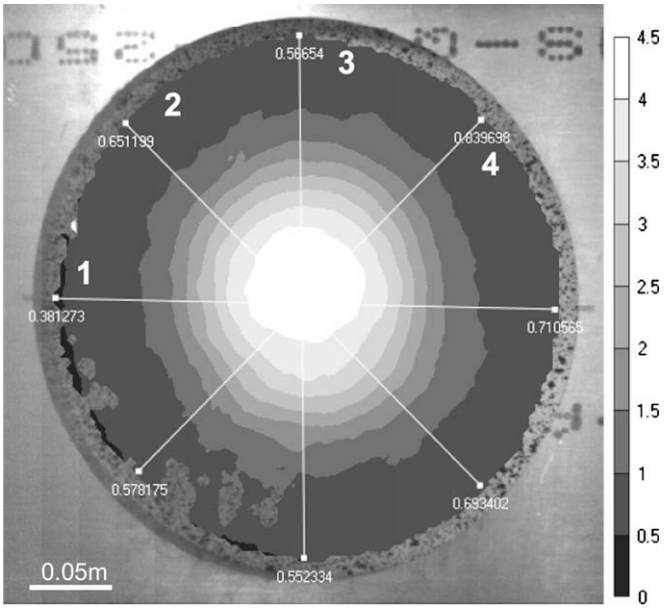

Fig. 6. Example full-field witness-plate deformation contour plot of out-of-plane deformation contours in mm, showing deformation symmetry and locations of the 4 diameters analyzed at the time of maximum deformation.

3.3. Description of material deformation

Qualitatively, the witness-plate motion is initiated by its midpoint acceleration, at the point of first shock incidence and maximum impulse. This motion drives the plate shape for approximately the first 500 μs of the event. Thereafter

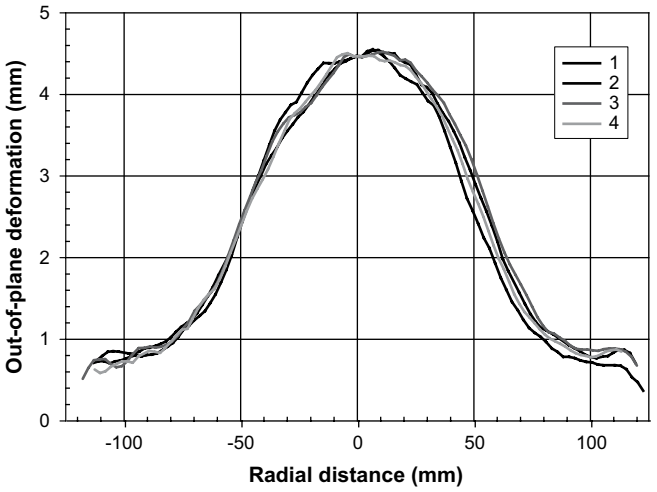

Fig. 7. Deformation measurements along witness-plate diameters, showing a high degree of symmetry about the point of maximum deformation. The exposed plate area is 0.25 m in diameter.

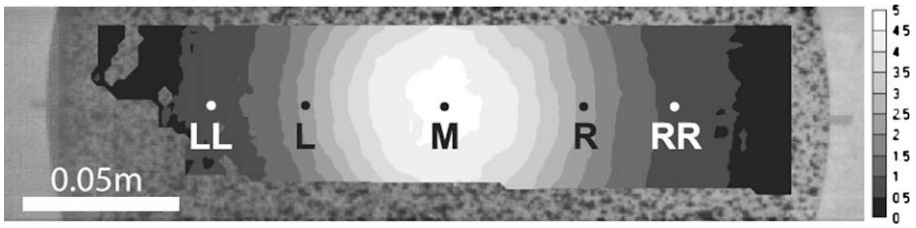

Fig. 8. Physical location of points used to examine plate deformation, showing out-of-plane deformation contours in mm at time $t = 167$ μs for TATP test #11.

a deformation wave, reflected from the circular shock-hole fixture boundary, dominates the plate motion and ultimately determines the final plate shape. This deformation wave is not considered further here, but has been examined by Hargather [23]. The present work focuses on measuring the initial maximum plate deformation, which is independent of the deformation wave reflection from the clamped boundary.

To analyze the initial plate motion, five physical locations on the witness-plate surface are identified as shown in Fig. 8: *LL*, *L*, *M*, *R*, *RR*. These five points are symmetrically positioned, with point *M* being the plate midpoint. The deformation contours shown in Fig. 8 are those at the time of maximum witness-plate deflection.

By analyzing the deformation-time history of each of these points, as shown in Fig. 9, the initial plate deformation process can be understood. The center of the plate, *M*, is accelerated first and, as it deforms, the remainder of the plate surface also begins to deform with it, starting at the innermost points *L* and *R*. The center point reaches its maximum deformation and then begins to move in the reverse direction. The other points reach their maximum deformations fractions of a millisecond later. The arrival of an in-plane deformation wave can be observed at points *LL* and *RR* at about $t = 0.3$ ms after the initial deformation. This deformation wave propagates toward the plate center and arrives at the next points, *L* and *R*, at about $t = 0.5$ ms. The deformation wave arrival is noted by the change in slope of the plate deformation at these times, but is more easily seen in Fig. 10.

Fig. 10 shows several deformation profiles across the witness-plate diameter during the first 667 μs of the explosive event. After reaching its maximum deformation at approximately time $t = 0.1$ ms in Fig. 9, the plate midpoint deflects back in the direction of the explosion, as also seen from Fig. 9. This is the beginning of plate oscillations that occur for approximately 10 ms before eventually damping and leaving the plate in its final deformation state.

After the plate has reached its initial maximum deformation, before the $t = 167$ μs curve in Fig. 10, a deformation wave enters the measurement region near the circular shock-hole fixture boundary, as noted above. This deformation wave appears to be a reflection from the clamped plate boundary. This wave grows in amplitude as it approaches the center of the plate. It can first be seen at $t = 333$ μs in Fig. 10, but is more clearly visible at the two later times shown in the figure. The deformation wave eventually reaches the center of the plate and decreases in amplitude, but continues to play an important role in the later plate deformation.

3.4. Dynamic deformation results

The observed maximum dynamic material response (e.g. at $t = 0.1$ ms in Fig. 9) is expected to scale according to the explosive impulse applied to the witness plate.

Data from the present shock-hole aluminum witness-plate deformation experiments are summarized in Table 1 for PETN and in Table 2 for TATP charges. These results include the actual mass and stand-off distance for each charge, which are then scaled in order to determine the impulse, as described in Section 2.3. The maximum impulse listed is the triangular impulse applied at the plate center. The average impulse is calculated by integrating the incident impulse over the entire plate surface for each experiment.

The maximum dynamic deformation data, plotted versus maximum impulse from Tables 1 and 2, are shown in Fig. 11. The same data are also shown in Fig. 12, zoomed in to better show the TATP results. The error bars in both figures represent the uncertainty in explosive impulse as shown earlier in Fig. 5. The error

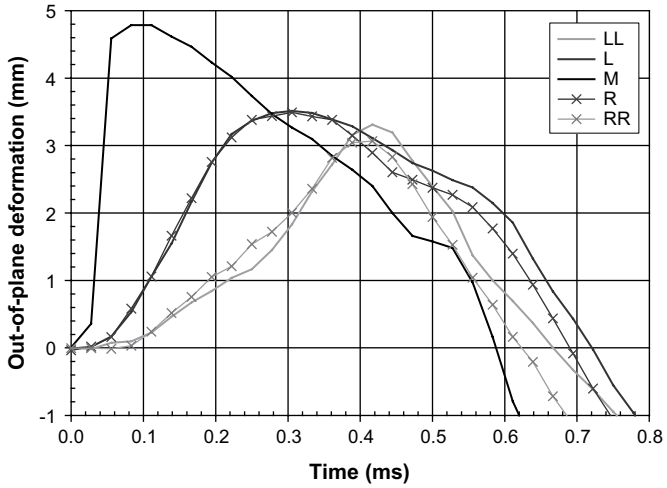

Fig. 9. Witness-plate deformation versus time for points along the plate surface, showing initial plate motion for TATP test #11.

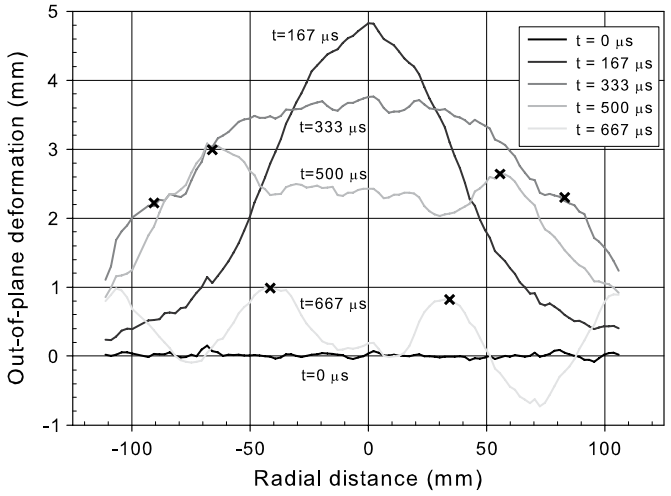

Fig. 10. Out-of-plane deformation versus time on the horizontal diameter of an aluminum witness plate during the first 667 μs of a typical test (TATP test #11), each X represents the approximate position of the deformation-wave crest.

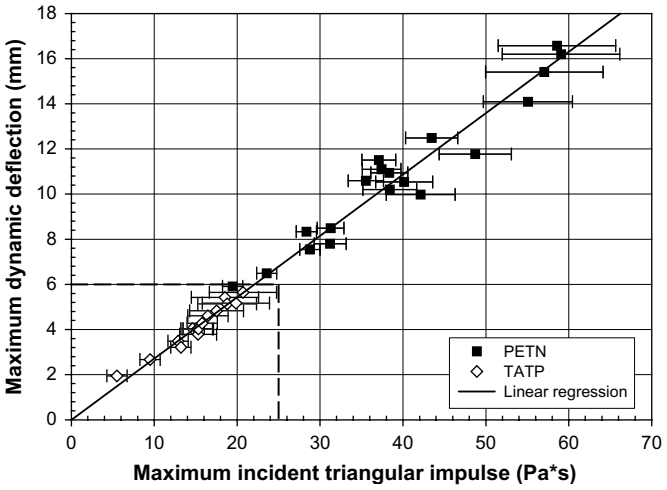

Fig. 11. Maximum dynamic witness-plate deformation versus maximum incident triangular explosive impulse (the region of Fig. 12 is shown by the dashed line).

increases with increasing impulse for each explosive material, which is a result of the characterization procedure [19]. The error in deformation measurement, as discussed in Section 3.2, is approximately ± 0.10 mm and is represented by the symbol size in Fig. 11.

Fig. 11 reveals one benefit of using more than one explosive material in these experiments: error reduction in the region of impulse overlap. The error for TATP at an impulse of 20 Pa s is large, but at the same impulse, PETN has a much smaller error bar (the error for TATP is larger because the TATP must be placed closer to the plate surface to obtain the same impulse). The present experimental data have increasing error at decreasing stand-off distance from the explosive, as discussed elsewhere [19,23]. Thus, measurement error can be minimized by conducting experiments at larger stand-off distances with larger charge masses.

The stand-off distance can be increased without limit, although at larger distances the shock wave becomes almost planar and impacts the entire plate surface at once. This change in plate loading affects the results but is not presently studied. The present results use both PETN and TATP charges across a range of stand-off distances limited to 0.15 m or less (Tables 1 and 2). By judiciously experimenting with various explosive materials, the range of applicability of each can be explored, while using the combined results to limit overall errors.

Fig. 13 shows the maximum plate deformation as a function of average incident explosive impulse. This figure is similar to Fig. 11, but shows a slightly different data collapse. A region of particular interest is for PETN tests 4–10, with maximum incident impulses from about 35–42 Pa s. This region has a distinct spread about the linear regression line in Fig. 11, but collapses almost perfectly in Fig. 13. This data collapse suggests that some degree of impulse averaging is appropriate.

The upper extreme of the PETN data in Fig. 13, however, appears to deviate from the linear regression when the impulse is simply averaged. This deviation suggests that a simple averaging is not appropriate for all stand-off distances. In particular, the data above an average impulse of 30 Pa s have a significantly higher deflection than expected by the linear fit. These experiments use a charge in close proximity to the plate, indicating that averaging over the entire plate surface is inappropriate, and that it is the localized loading that is driving the witness-plate center response. At present, the deviation is still within the experimental error, so further averaging schemes are not presented here. Future experimental and computational investigations of the effect of impulse variation and averaging will be carried out.

Overall, the regressions shown in Figs. 11–13 highlight the approximately-linear relationship between maximum witness-plate dynamic deflection and explosive impulse. The regression was forced to pass through the coordinate origin to maintain physical realism. This linear relationship is valid for the present data on aluminum witness plates, but is not expected to be applicable outside of the present data range, especially when material failure is approached.

4. Recommendations for future work

This laboratory-scale approach to materials blast testing and research can be used in various ways to extend the current understanding of high-speed material responses. The present work has explored only a single aluminum alloy's response to a limited range of blast impulses, given as a baseline example. The work could first be extended to explore the impulse-deformation trend as the present aluminum witness-plate approaches failure. Measuring and studying the strain and strain-rate distributions across the plate surface as failure occurs could improve current material and fracture models. The strain-rate profiles could also be used to estimate the energy absorbed by the witness plate, relative to the shock energy that is reflected and transmitted. Similar

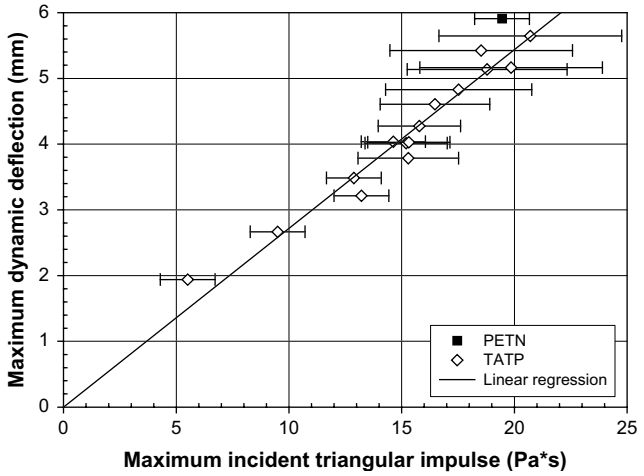

Fig. 12. Maximum dynamic witness-plate deformation versus maximum incident triangular explosive impulse, detail.

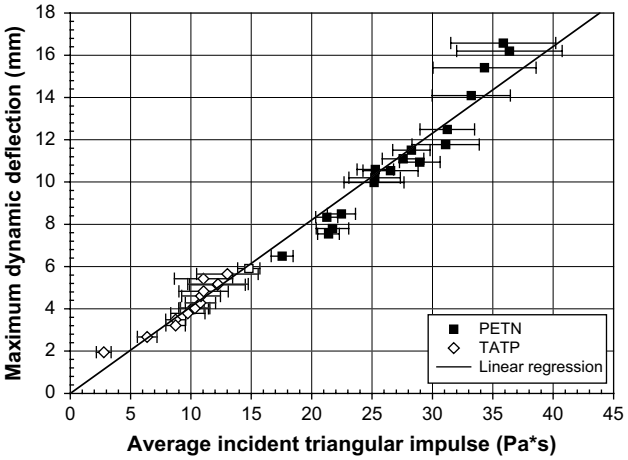

Fig. 13. Maximum dynamic witness-plate deformation versus average incident triangular explosive impulse.

research conducted with witness plates of various thicknesses and exposed surface areas would build a broader understanding of the scaling of material responses. Ultimately the techniques can be applied to exotic materials to explore the range of non-linear loading responses produced by novel materials. These comparatively-inexpensive laboratory experiments can thus be used to scale material responses and to estimate full-scale results before conducting expensive full-scale experiments.

These techniques are also well-suited to compliment computational simulations. They provide high-resolution experimental data, with known and highly-controlled boundary conditions, which are ideal for computational code validation. Such experimental results could be used to validate material models or blast computations on a small-scale experiment before modeling a full-scale problem. Laboratory-scale experimental blast data could also be used to inversely determine non-linear and rate-dependent material properties of aluminum or of novel blast-resistant materials.

5. Conclusions

A new method is presented to conduct quantitative material blast experiments in the laboratory. The approach focused on developing a detailed understanding of the applied explosive load and the resulting material deformation. It was shown that the maximum deformation of simple aluminum witness plates, clamped in a shock-hole fixture, scales according to the applied explosive impulse, as determined from an explosive characterization.

The use here of two different previously-characterized explosives has improved the understanding of the explosive loading during a material blast experiment. The technique of propagating the explosively-driven shock wave through air before impacting the witness plate is new to the present work. Through this approach, the exact loading conditions on the plate are well known, and can thus be used directly to scale results or validate computational models.

A linear impulse-deformation relationship was found for the present experiments, as previously reported elsewhere [27]. However, the ability to scale material deformations across explosions of different materials is a new result presented here. This scaling ability is directly related to the ability to characterize explosives through the procedure developed by Hargather and Settles [19]. Approximating the impulse loading by a triangular impulse was also shown to be appropriate for generating this simple relationship between deformation and loading. The approximation can further be used to define an incident impulse or an average impulse over the plate, both of which are broadly appropriate for deformation scaling. An average impulse calculation is likely the most appropriate, although more experimentation must be done to explore the appropriate averaging relationship and limits based on the physical charge dimensions and location.

Optical techniques, used here to measure the material deformation throughout explosive events, produce a large volume of experimental data. The present paper is focused solely on measuring time-resolved deformation. However, the data can also be analyzed to yield stress-strain relationships across the witness-plate surface, and to contribute to the development of complex material-property models.

The experiments performed here were done safely and economically in the ordinary laboratory environment. Optical diagnostics, typically not amenable to large-scale outdoor experiments, were used to measure detailed full-field material responses to explosive loading.

References

[1] Houlston R, Slater JE, Pegg N, DesRochers GG. On analysis of structural response of ship panels subjected to air blast loading. Comput Struct 1985;21:273–89.
[2] Jacinto AC, Ambrosini RD, Danesi RF. Experimental and computational analysis of plates under air blast loading. Int J Impact Eng 2001;25:927–47.
[3] Settles GS. Schlieren and shadowgraph techniques. New York: Springer-Verlag; 2001.
[4] Nurick GN, Martin JB. Deformation of thin plates subjected to impulsive loading – A review .2. Experimental studies. Int J Impact Eng 1989;8:171–86.
[5] Nurick GN, Gelman ME, Marshall NS. Tearing of blast loaded plates with clamped boundary conditions. Int J Impact Eng 1996;18:803–27.
[6] Stoffel M, Schmidt R, Weichert D. Shock wave-loaded plates. Int J Solids Struct 2001;38:7659–80.
[7] Neuberger A, Peles S, Rittel D. Scaling the response of circular plates subjected to large and close-range spherical explosions. Part I: air-blast loading. Int J Impact Eng 2007;34:859–73.
[8] Turkmen HS. Structural response of laminated composite shells subjected to blast loading: comparison of experimental and theoretical methods. J Sound Vib 2002;249:663–78.
[9] Nurick GN, Martin JB. The measurement of the response of clamped circular plates to impulsive loading. Inst Phys Conf Ser 1984;70:495–502.
[10] Espinosa H, Mello M, Xu Y. Desensitized displacement interferometer applied to impact recovery experiments. Appl Phys Lett 1996;69:3161–3.
[11] Espinosa H, Lee S, Moldovan N. A novel fluid structure interaction experiment to investigate deformation of structural elements subjected to impulsive loading. Exp Mech 2006;46:805–24.
[12] Siebert T, Becker T, Spiltthof K, Neumann I, Krupka R. High-speed digital image correlation: error estimations and applications. Opt Eng 2007;46.
[13] Forney WL, Leiste U, Bonenberger R, Goodings D. Explosive impulse on plates. Fragblast 2005;9:1–17.
[14] Forney WL, Leiste U, Bonenberger R, Goodings D. Mechanism of loading on plates due to explosive detonation. Fragblast 2005;9:205–17.
[15] Tiwari V, Sutton MA, McNeill SR. Assessment of high speed imaging systems for 2D and 3D deformation measurements: methodology development and validation. Exp Mech 2007;47:561–79.
[16] Bodner SR, Symonds PS. Experiments on viscoplastic response of circular plates to impulsive loading. J Mech Phys Solids 1979;27:91–113.
[17] Teelingsmith RG, Nurick GN. The deformation and tearing of thin circular plates subjected to impulsive loads. Int J Impact Eng 1991;11:77–91.
[18] Wierzbicki T, Nurick GN. Large deformation of thin plates under localised impulsive loading. Int J Impact Eng 1996;18:899–918.
[19] Hargather MJ, Settles GS. Optical measurement and scaling of blasts from gram-range explosive charges. Shock Waves 2007;17:215–23.
[20] Kleine H, Dewey JM, Ohashi K, Mizukaki T, Takayama K. Studies of the TNT equivalence of silver azide charges. Shock Waves 2003;13:123–38.
[21] Bonorchis D, Nurick G. The influence of boundary conditions on the loading of rectangular plates subjected to localised blast loading – importance in numerical simulations. Int J Impact Eng 2009;36:40–52.
[22] Correlated Solutions Inc., Vic-3D User Manual; 2006.
[23] Hargather MJ. Scaling, characterization and application of gram-range explosive charges to blast testing of materials. PhD thesis, Pennsylvania State University, Department of Mechanical and Nuclear Engineering; 2008.
[24] Kinney GF, Graham KJ. Explosive shocks in air. New York: Springer-Verlag; 1985.
[25] Baker WE. Explosions in air. Austin: University of Texas Press; 1973.
[26] Dewey JM. Expanding spherical shocks (blast waves). In: Ben-Dor G, Igra O, Elperin E, editors. Handbook of shock waves, vol. 2. San Diego: Academic Press; 2001. p. 441–81.
[27] Bonorchis D, Nurick G. The effect of welded boundaries on the response of rectangular hot-rolled mild steel plates subjected to localised blast loading. Int J Impact Eng 2007;34:1729–38.